

## DISCOVERY OF 35 NEW SUPERNOVA REMNANTS IN THE INNER GALAXY

C. L. BROGAN<sup>1</sup>, J. D. GELFAND<sup>2</sup>, B. M. GAENSLER<sup>2</sup>, N. E. KASSIM<sup>3</sup>, T. J. LAZIO<sup>3</sup>

*Draft version August 4, 2021*

### ABSTRACT

We report the discovery of up to 35 new supernova remnants (SNRs) from a 42'' resolution 90cm multi-configuration Very Large Array survey of the Galactic plane covering  $4.5^\circ < \ell < 22.0^\circ$  and  $|b| < 1.25^\circ$ . Archival 20cm, 11cm, and 8  $\mu$ m data have also been used to identify the SNRs and constrain their properties. The 90cm image is sensitive to SNRs with diameters 2.5' to 50' and down to a surface brightness limit of  $\sim 10^{-21} \text{ W m}^{-2} \text{ Hz}^{-1} \text{ sr}^{-1}$ . This survey has nearly tripled the number of SNRs known in this part of the Galaxy, and represents an overall 15% increase in the total number of Galactic SNRs. These results suggest that further deep low frequency surveys of the inner Galaxy will solve the discrepancy between the expected number of Galactic SNRs and the significantly smaller number of currently known SNRs.

*Subject headings:* ISM:supernova remnants – radio continuum:ISM – surveys

### 1. INTRODUCTION

Statistical studies of supernova (SN) rates, based on OB star counts, pulsar birth rates, Fe abundance, and the SN rate in other Local Group galaxies, suggest that there should be many more supernova remnants (SNRs) in our Galaxy ( $\gtrsim 1000$ ; Li et al. 1991; Tammann, Loeffler, & Schroeder 1994) than are currently known ( $\sim 231$ ; Green 2004). This deficit is likely the result of selection effects acting against the discovery of old, faint, large remnants, as well as young, small remnants in previous low resolution and/or poor sensitivity Galactic radio surveys (e.g. Green 1991). For example, past single dish surveys with  $\lambda \geq 11$  cm have resolutions  $> 4'$  (e.g. Haslam et al. 1982; Reich, Reich, & Fürst 1990). The 20cm NRAO Very Large Array (VLA) Sky Survey (NVSS) has high resolution ( $\sim 45''$ ) but poor surface brightness sensitivity (Condon et al. 1998). The missing remnants are likely concentrated toward the inner Galaxy where the diffuse Galactic plane synchrotron emission and thermal H II regions cause the most confusion. This premise is supported by the large number of new SNRs discovered in the 4th quadrant by Whiteoak & Green (1996) using the Molonglo Observatory Synthesis Telescope (MOST) at 35cm with  $\sim 45''$  resolution and comparatively high sensitivity. Despite the success of the MOST survey, a significant shortfall compared to predictions remains – most likely due to limited dynamic range.

Thus, more sensitive, high resolution surveys of the inner Galaxy at low radio frequencies are the key to determining whether the “missing” remnants exist or if our understanding of SN rates is significantly flawed. From multi-configuration VLA 90cm (330 MHz) observations of just 1 deg<sup>2</sup> centered on SNR G11.2-0.3, Brogan et al. (2004) discovered three new SNRs, demonstrating the power of such observations. This Letter presents the discovery of 35 SNRs (including the three described above) from a more extensive 90cm VLA survey.

### 2. OBSERVATIONS AND RESULTS

We have imaged the Galactic plane at 90cm from  $\ell = +4.5^\circ$  to  $+22^\circ$  and  $|b| < 1.25^\circ$  using the VLA in the B, C, and

D configurations between 2002 and 2004. The VLA 90cm FWHM primary beam is  $2.5^\circ$  and the mosaiced image is comprised of 14 pointings, each separated by  $\sim 1.25^\circ$ . The majority of these data are new, but VLA archival data are also included for regions near  $\ell = 6^\circ, 9^\circ, 11^\circ, \& 21^\circ$ . Each pointing was observed for approximately 1.2, 1.6, and 2.2 hours in the D, C, and B configurations, respectively, over a wide range of hour angles. The data were reduced using AIPS and standard wide-field, low frequency data reduction techniques<sup>4</sup> (e.g. Brogan et al. 2004).

In order to achieve high resolution images that are also sensitive to extended structure, we have employed the multi-scale (MS) cleaning algorithm in AIPS (e.g. Wakker & Schwarz 1988). Instead of a point source clean model, MS clean tapers the data and cleans on a variety of scales; this process virtually eliminates artifacts due to the “clean instability”. Three scales were used to create the 90cm mosaic: the intrinsic resolution of the multi-configuration data of  $\sim 40'' \times 30''$  (differing slightly for each pointing),  $100''$ , and  $220''$ . After cleaning, the individual images were convolved to a common resolution of  $42''$ , corrected for primary beam attenuation, and then linearly mosaiced. These data are not sensitive to structures  $\gtrsim 50'$ , and thus resolve out the Galactic background synchrotron emission. The final rms noise of the mosaiced image is a function of  $b$  and is  $\sim 5 \text{ mJy beam}^{-1}$  for  $|b| \lesssim 0.5^\circ$ , increasing to  $\sim 8 \text{ mJy beam}^{-1}$  at  $|b| = 1^\circ$ . This is by far the highest dynamic range large-scale image<sup>5</sup> of this part of the Galactic plane yet created for  $\lambda > 20$ cm.

Complementary images at other frequencies are required to search for non-thermal emission. For this purpose we have created a 20cm mosaic of a large fraction of the 90cm survey region using data from the northern extension of the Southern Galactic Plane Survey (SGPS) observed with the Australia Telescope Compact Array (see McClure-Griffiths et al. 2005, survey region includes  $5^\circ < \ell < 20^\circ$ ) combined with archival VLA D-configuration 20cm data (see Helfand et al. 2005b, outside the SGPS region the VLA data alone were used). The resolution of this image is  $70'' \times 37''$  and the rms noise is  $\sim 15 \text{ mJy beam}^{-1}$ . The resulting 20cm image is not sensitive to smooth structures larger than about  $\sim 18'$ , for this reason the 4/3 resolution single dish Bonn 11cm survey

<sup>1</sup> Institute for Astronomy, 640 North A'ohoku Place, Hilo, HI 96720; cbrogan@ifa.hawaii.edu.

<sup>2</sup> Harvard-Smithsonian Center for Astrophysics, 60 Garden Street, Cambridge, MA 02138

<sup>3</sup> Remote Sensing Division, Naval Research Laboratory, Washington DC 20375-5351

<sup>4</sup> Described at <http://www.vla.nrao.edu/astro/guides/p-band/>

<sup>5</sup> Image is available from C. Brogan upon request.

data with an rms noise of  $\sim 8$  mJy beam $^{-1}$  were also utilized (Reich, Reich, & Fürst 1990). *Midcourse Space Experiment* (MSX) 8  $\mu$ m data (Price et al. 2001) with 20'' resolution were also used to distinguish between thermal and non-thermal emission (non-thermal emission is anti-correlated with bright IR emission).

### 2.1. SNR Candidates

The SNR candidates were selected based on the following criteria:

1. The source must be resolved in our 42'' 90cm image and show a shell-like (or partial shell) morphology
2. The radio continuum spectral index ( $S_\nu \propto \nu^\alpha$ ) computed from the integrated flux densities must be negative, indicative of non-thermal emission
3. The source must be distinct from bright mid-IR 8  $\mu$ m emission.

Table 1 lists the 35 sources that meet these criteria. By way of confirmation, this list includes seven sources that have been previously identified as SNR candidates that have not yet been included in Green’s SNR catalog (Green 2004). The 19 previously identified SNRs within the survey region are also detected and confirmed (see Green 2004).

For the determination of criterion two both the 20 and 11cm flux density estimates suffer from significant caveats. The 20cm flux densities ( $S_{20\text{cm}}$ ) for candidates larger than about 10' are likely to be lower limits (due to missing short spacing information);  $S_{20\text{cm}}$  measurements for candidates larger than  $\sim 18'$  are precluded. The 11cm flux densities suffer to varying degrees from confusion due to the comparably low resolution of this survey. The flux densities at all three wavelengths have been corrected for background emission, though this correction is least certain for the 11cm data. For the majority of candidates, the spectral indices ( $\alpha$ ) determined from the 90/20 cm data and 90/11 cm data (last two columns of Table 1) are in good agreement.

The third criterion is useful in eliminating optically thick H II regions and thermal wind blown bubbles (WBB). Although the continuum emission from most WBBs is thermal (i.e. no SN has happened inside the bubble), they tend to have flat spectra and shell like morphologies that are not easily distinguished from SNRs. However, WBB (and H II regions) are also invariably surrounded by a shell of bright 8  $\mu$ m emission. While SNRs can also have associated mid-IR emission (e.g. Reach et al. 2005), this emission tends to be weak and often undetectable at the sensitivity of *MSX*. Three-color images of the W30 and W28 regions are shown in Figure 1a,b to demonstrate both the high quality of the 90cm image and the candidate search technique.

Each candidate in Table 1 has been assigned a ‘‘class’’ of I, II, or III: (I) we are very confident that the source is an SNR and all three flux measurements are believed accurate; (II) we are fairly confident that the source is an SNR, but the candidate is either confused with thermal emission and especially the 11cm flux density is uncertain or the source is large enough that the 20cm flux density could not be estimated with the current data – higher resolution and sensitivity follow-up is desirable; (III) the candidate is coincident with non-thermal emission but it is very faint, very confused, or does not exhibit a typical shell type SNR morphology and future follow-up is

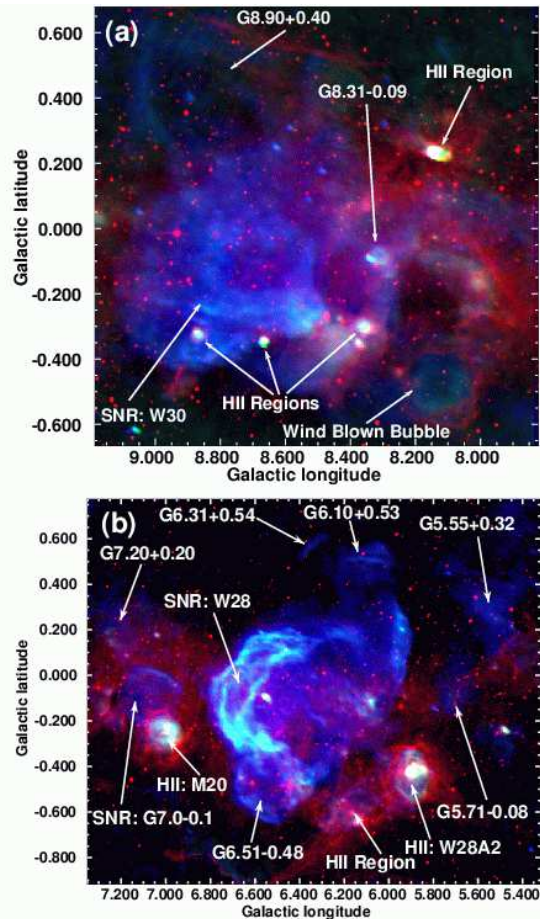


FIG. 1.— Three color images with *blue*=VLA 90cm, *red*=MSX 8  $\mu$ m, and *green*=SGPS+VLA 20cm of the (a) W30 region and (b) W28 region. New SNRs are indicated using Galactic coordinates; the previously known SNRs, H II regions, and a WBB are also labeled.

essential. There are 15 class-I, 16 class-II, and 4 class-III candidates. Hereafter, all 35 sources will be designated as SNRs; images of the new SNRs at 90cm are shown in Figure 2 (except for the three described in Brogan et. al (2004)). Six of the new SNRs are coincident with possible ASCA X-ray counterparts as indicated in Table 1; no pulsars are coincident with any of the new SNRs based on the Manchester et al. (2005) catalog.

Helfand et al. (2005b) recently reported the discovery of 30 SNR candidates in the same region described in this work as part of their larger Multi-Array Galactic Plane Imaging Survey (MAGPIS; the latitude extent is  $|b| < 0.8^\circ$ ). Applying the criteria listed in §2.1, we find supporting evidence that 15 of the Helfand et al. (2005b) sources are SNRs. The 15 candidates in common between the two surveys are indicated in Table 1. The Helfand et al. (2005b) 20cm integrated flux densities are typically  $\sim 4$  times higher than those listed in Table 1 because their measurements were not restricted to the candidate’s spatial extent nor was background subtraction performed.

### 3. DISCUSSION

Generally, the SNRs discovered in this survey are smaller and fainter than those previously known in this region. The mean and median diameters of the new SNRs are  $\sim 12'$  and  $8'$ . The SNR candidates have 1 GHz surface brightnesses in the range  $\Sigma_{1\text{GHz}} = (1-15) \times 10^{-21}$  W m $^{-2}$  Hz $^{-1}$  sr $^{-1}$ . This result suggests that the Bonn 11cm completeness limit estimated by

TABLE 1  
PROPERTIES OF SNR CANDIDATES

$\ell$ ( $^{\circ}$ )	$b$ ( $^{\circ}$ )	R. A. (h m s)	Dec. ( $^{\circ}$ ' )	Size ( $'$ x $'$ )	Morphology <sup>a</sup>	Class	$S_{90\text{cm}}^b$ (Jy)	$S_{20\text{cm}}^b$ (Jy)	$S_{11\text{cm}}^b$ (Jy)	$\alpha_{(90/20)}^c$	$\alpha_{(90/11)}^c$	Notes <sup>d</sup>
5.55	+0.32	17 57 04	-24 00	12 x 15	Shell	II	14.3 (0.3)	4.6 (0.9)	3.9 (0.4)	-0.8	-0.6	
5.71	-0.08	17 58 49	-24 03	9 x 12	Partial Shell	III	4.3 (0.2)	2.0 (0.6)	1.6 (0.2)	-0.5	-0.5	
6.10	+0.53	17 57 29	-23 25	18 x 12	Partial Shell	I	13.4 (0.2)	3.5 (0.7)	2.0 (0.2)	-0.9	-0.9	
6.31	+0.54	17 57 54	-23 14	3 x 9	Filament	III	1.4 (0.1)	0.7 (0.3)	0.3 (0.1)	-0.5	-0.8	
6.51	-0.48	18 02 11	-23 34	18 x 18	Shell	I	60.8 (0.4)	22.1 (1.1)	22.7 (2.3)	-0.7	-0.5	H/O
7.20	+0.20	18 01 07	-22 38	12 x 12	Partial Shell	II	5.2 (0.2)	2.3 (0.7)	1.8 (0.2)	-0.6	-0.5	H
8.31	-0.09	18 04 34	-21 49	5 x 4	Shell	II	2.3 (0.1)	1.0 (0.2)	0.5 (0.1)	-0.6	-0.7	H
8.90	+0.40	18 03 58	-21 03	24 x 24	Shell	II	18.2 (0.5)	...	4.9 (0.5)	...	-0.6	
9.70	-0.06	18 07 22	-20 35	15 x 11	Shell	I	6.5 (0.2)	3.0 (0.7)	1.5 (0.2)	-0.5	-0.7	H
9.95	-0.81	18 10 41	-20 43	12 x 12	Shell	II	11.0 (0.3)	5.9 (0.8)	4.6 (0.5)	-0.4	-0.4	
10.59	-0.04	18 09 08	-19 47	6 x 6	Partial Shell	II	1.4 (0.1)	0.7 (0.3)	0.3 (0.1)	-0.5	-0.7	X
11.03	-0.05	18 10 04	-19 25	9 x 11	Partial Shell	I	3.1 (0.2)	1.1 (0.5)	1.0 (0.1)	-0.7	-0.5	O/X
11.15	-0.71	18 12 46	-19 38	11 x 7	Partial Shell	I	2.3 (0.1)	0.8 (0.4)	0.4 (0.1)	-0.7	-0.8	H/O
11.17	-1.04	18 14 03	-19 46	18 x 12	Shell	I	11.0 (0.3)	4.7 (0.8)	4.1 (0.4)	-0.6	-0.5	O
11.18	+0.11	18 09 47	-19 12	12 x 10	Shell	I	3.5 (0.2)	2.0 (0.5)	1.6 (0.2)	-0.4	-0.4	H/O
11.89	-0.21	18 12 25	-18 44	4 x 4	Shell	II	0.9 (0.1)	0.6 (0.2)	0.4 (0.1)	-0.3	-0.4	H/X
12.26	+0.30	18 11 17	-18 10	5 x 6	Partial Shell	I	1.5 (0.1)	0.6 (0.3)	0.4 (0.1)	-0.7	-0.6	H
12.58	+0.22	18 12 14	-17 55	5 x 6	Composite?	II	0.8 (0.1)	0.5 (0.3)	0.3 (0.1)	-0.4	-0.5	
12.72	-0.00	18 13 19	-17 54	6 x 6	Shell	I	2.0 (0.1)	0.6 (0.3)	0.3 (0.1)	-0.8	-0.8	H
12.83	-0.02	18 13 37	-17 49	3 x 3	Shell	I	1.2 (0.1)	0.7 (0.2)	0.4 (0.1)	-0.4	-0.5	H/O/X
14.18	-0.12	18 15 52	-16 34	6 x 5	Shell	II	0.9 (0.1)	0.4 (0.3)	0.3 (0.1)	-0.6	-0.5	
14.30	+0.14	18 15 58	-16 27	5 x 4	Partial Shell	II	1.2 (0.1)	0.5 (0.3)	0.6 (0.1)	-0.5	-0.3	
15.42	+0.18	18 18 02	-15 27	14 x 15	Shell	I	10.9 (0.3)	4.6 (0.8)	2.9 (0.3)	-0.6	-0.6	
15.51	-0.15	18 19 25	-15 32	8 x 9	Shell	III	4.2 (0.2)	1.9 (0.5)	1.0 (0.1)	-0.5	-0.7	
16.05	-0.57	18 21 56	-15 14	15 x 10	Shell	I	4.9 (0.2)	2.2 (0.7)	1.3 (0.1)	-0.6	-0.6	
16.41	-0.55	18 22 38	-14 55	13 x 13	Partial Shell	II	10.0 (0.3)	3.6 (0.9)	2.0 (0.2)	-0.7	-0.8	
17.02	-0.04	18 21 57	-14 08	5 x 5	Shell	I	0.7 (0.1)	0.4 (0.3)	0.3 (0.1)	-0.5	-0.4	H
17.48	-0.12	18 23 08	-13 46	6 x 6	Partial Shell	II	0.9 (0.1)	0.3 (0.4)	0.3 (0.1)	-0.7	-0.6	
18.16	-0.16	18 24 34	-13 11	8 x 8	Shell	I	7.6 (0.1)	3.9 (0.4)	3.0 (0.3)	-0.5	-0.4	H/O/X
18.62	-0.28	18 25 55	-12 50	6 x 6	Partial Shell	II	1.9 (0.1)	1.2 (0.4)	0.7 (0.1)	-0.3	-0.5	H
19.13	+0.90	18 22 37	-11 50	24 x 18	Partial Shell	III	27.2 (0.5)	...	9.4 (0.9)	...	-0.5	
19.15	+0.27	18 24 56	-12 07	27 x 27	Partial Shell	II	17.4 (0.4)	...	5.5 (0.6)	...	-0.5	
20.47	+0.16	18 27 51	-11 00	8 x 8	Shell	I	4.2 (0.1)	2.7 (0.4)	1.4 (0.1)	-0.3	-0.5	H
21.04	-0.47	18 31 12	-10 47	9 x 7	Shell	II	2.3 (0.2)	0.9 (0.5)	0.5 (0.1)	-0.6	-0.7	
21.56	-0.10	18 30 50	-10 09	5 x 5	Partial Shell	II	0.5 (0.1)	0.3 (0.2)	0.2 (0.1)	-0.4	-0.6	H/X

<sup>a</sup>“Partial shell” morphology indicates that  $\lesssim 70\%$  of a complete shell is evident in the 90cm image.

<sup>b</sup>Statistical uncertainties are provided in parenthesis, for the 90 and 21cm data they are calculated from  $(\# \text{ independent beams})^{0.5} \times 3\sigma$ , while it is the larger of  $10\sigma$  or  $10\%$  for the 11cm data.

<sup>c</sup>Spectral indices between indicated wavelengths using  $S_{\nu} \propto \nu^{\alpha}$ ; the uncertainty in  $\alpha$  is typically the larger of  $|\alpha_{(90/20)} - \alpha_{(90/11)}|$  or 0.2.

<sup>d</sup>H: also candidate in Helfand et al. (2005b). O: previously reported in (ascending  $\ell$  order) Yusef-Zadeh et al. (2000); Brogan et al. (2004); Brogan et al. (2004); Trushkin (1996); Brogan et al. (2004); both Brogan et al. (2005) and Helfand et al. (2005a); Odegard (1986). X: Possible ASCA X-ray counterpart in Sugizaki et al. (2001) or Bamba et al. (2003).

Green (2004) of  $\sim 10^{-20} \text{ W m}^{-2} \text{ Hz}^{-1} \text{ sr}^{-1}$  is accurate and that the current survey is  $\sim 10$  times deeper.

This limited 90cm survey of  $42.5 \text{ deg}^2$  has produced a  $\sim 15\%$  increase in the total number of known Galactic SNRs. The number of identified remnants within the survey boundaries (previously 19) has increased by nearly a factor of 3 to 54. Based on completeness considerations and empirical evidence, respectively, Helfand et al. (1989) and Brogan et al. (2004) estimate that there should be between 65 to 85 SNRs in this region, in reasonable agreement with the observed number, given that we are insensitive to the smallest ( $\lesssim 2.5'$ ) and largest ( $\gtrsim 0.8^{\circ}$ ) size scale remnants, as well as Crab like remnants lacking radio shells.

To estimate the implications of these new SNR discoveries on the total number of Galactic SNRs we assume (1) the current SNR catalog (Green 2004) is essentially complete for  $|b| > 1.25^{\circ}$  and for  $|\ell| > 50^{\circ}$ ; (2) that the Bonn 11cm survey in the 1st quadrant and the MOST 35cm survey in the 4th quadrant have similar levels of completeness (e.g. Green 2004); and (3) the number of known SNRs between  $|b| < 1.25^{\circ}$  and  $|\ell| < 50^{\circ}$  (115) should be scaled by a factor of three (i.e. the increase achieved in our limited survey). The

$\ell = 50^{\circ}$  cutoff is guided by the longitude extent of the inner Galactic disk. These assumptions result in a prediction of 460 for the number of Galactic SNRs, still a factor of two less than the expected  $\sim 1,000$  SNRs (see §1).

However, five of the new SNRs are in close proximity to (or coincident with) the two largest previously known SNRs in the survey region: W28 and W30 (Figs. 1a,b), but appear distinct from them. Although we do not currently know if the new SNRs are physically close to the two known SNRs (along the line of sight), such a result would be unsurprising since high mass stars form in clustered environments. A new SNR has also been proposed to lie along the line of sight to the Vela SNR (i.e. G266.2-1.2 Aschenbach 1998). Such superpositions throughout the plane may also explain some fraction of the “missing” remnants. The assumption of completeness for  $|\ell| > 50^{\circ}$  is also probably flawed as a few SNRs continue to be discovered in the outer Galaxy (e.g. Kothes et al. 2001).

Overall, these results suggest that the “missing SNRs” problem can be attributed to selection effects and not our understanding of SN rates. Future instruments like the EVLA, LWA, ATA, and SKA will allow even deeper low frequency, high dynamic range surveys which will likely discover the re-

maining shortfall of Galactic SNRs.

The National Radio Astronomy Observatory operates the Very Large Array and is a facility of the National Science Foundation operated under a cooperative agreement by Asso-

ciated Universities, Inc. This research made use of data products from the Midcourse Space Experiment. Basic research in radio astronomy at the NRL is supported by the Office of Naval Research. We would also like to thank the SGPS team for their hard work in acquiring the ATCA 20cm data.

#### REFERENCES

- Aschenbach, B. 1998, *Nature*, 396, 141
- Bamba, A., Ueno, M., Koyama, K., & Yamauchi, S. 2003, *ApJ*, 589, 253
- Brogan, C. L., Gaensler, B. M., Gelfand, J. D., Lazendic, J. S., Lazio, T. J. W., Kassim, N. E., & McClure-Griffiths, N. M. 2005, *ApJ*, 629, L105
- Brogan, C. L., Devine, K. E., Lazio, T. J., Kassim, N. E., Tam, C. R., Briske, W. F., Dyer, K. K., & Roberts, M. S. E. 2004, *AJ*, 127, 355
- Condon, J. J., Cotton, W. D., Greisen, E. W., Yin, Q. F., Perley, R. A., Taylor, G. B., & Broderick, J. J. 1998, *AJ*, 115, 1693
- Green, D. A. 1991, *PASP*, 103, 209
- Green, D. A. 2004, *Bull. Astro. Soc. India*, 32, 335
- Haslam, C. G. T., Stoffel, H., Salter, C. J., & Wilson, W. E. 1982, *A&AS*, 47, 1
- Helfand, D.J., Becker, R.H., & White, R.L., astro-ph/0505392
- Helfand, D.J., Becker, R.H., White, R.L., Fallon, A., and Tuttle, S., astro-ph/0510468
- Helfand, D. J., Velusamy, T., Becker, R. H., & Lockman, F. J. 1989, *ApJ*, 341, 151
- Kothes, R., Landecker, T. L., Foster, T., & Leahy, D. A. 2001, *A&A*, 376, 641
- Li, Z., Wheeler, J. C., Bash, F. N., & Jefferys, W. H. 1991, *ApJ*, 378, 93
- Manchester, R. N., Hobbs, G. B., Teoh, A., & Hobbs, M. 2005, *AJ*, 129, 1993
- McClure-Griffiths, N. M., Dickey, J. M., Gaensler, B. M., Green, A. J., Haverkorn, M., & Strasser, S. 2005, *ApJS*, 158, 178
- Odegard, N. 1986, *AJ*, 92, 1372
- Price, S. D., Egan, M. P., Carey, S. J., Mizuno, D. R., & Kuchar, T. A. 2001, *AJ*, 121, 2819
- Reach et al. 2005, accepted to *AJ*, astro-ph/0510630
- Reich, W., Reich, P., & Fürst, E. 1990, *A&AS*, 83, 539
- Sugizaki, M., Mitsuda, K., Kaneda, H., Matsuzaki, K., Yamauchi, S., & Koyama, K. 2001, *ApJS*, 134, 77
- Tammann, G. A., Loeffler, W., & Schroeder, A. 1994, *ApJS*, 92, 487
- Trushkin, S. A. 1996, *Bull. Special Astrophys. Obs.*, 41, 64
- Wakker, B. P., & Schwarz, U. J. 1988, *A&A*, 200, 312
- Whiteoak, J. B. Z., & Green, A. J. 1996, *A&AS*, 118, 329
- Yusef-Zadeh, F., Shure, M., Wardle, M., & Kassim, N. 2000, *ApJ*, 540, 842

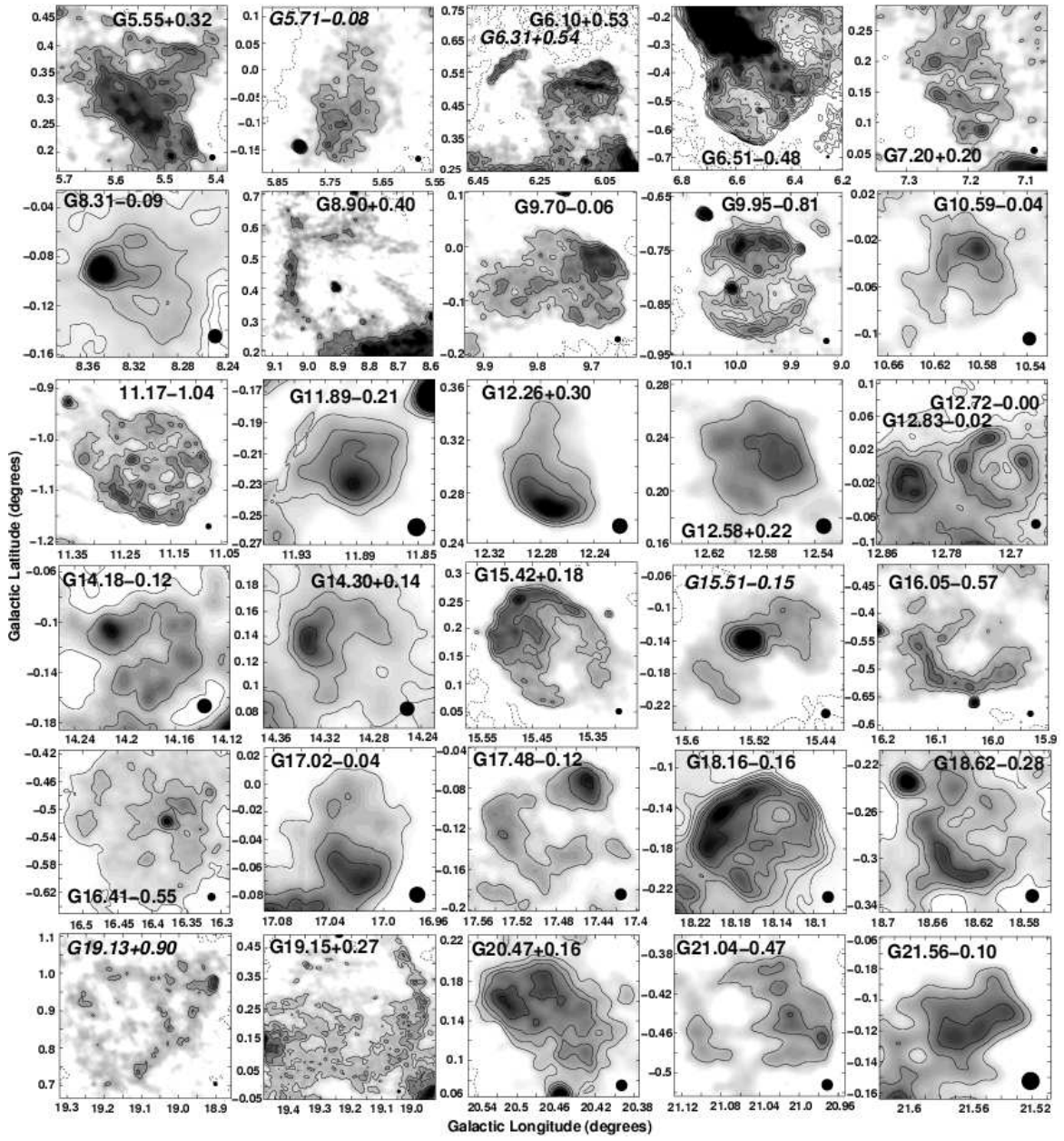


FIG. 2.— VLA 90cm images of the newly discovered SNRs (excluding three shown in Brogan et al. (2004)). The contour levels on each image are  $-25, 25, 37.5, 50, 75, 100, \& 125 \text{ mJy beam}^{-1}$ . For latitudes  $|b| \lesssim 0.5^\circ$ ,  $25 \text{ mJy beam}^{-1}$  is approximately  $5\sigma$ , while it is  $\sim 3\sigma$  at higher latitudes. The resolution of these images is  $42''$ ; the beam size is shown in the lower right of each panel for comparison. Class III sources are labeled in italics.